New isotope ^{276}Ds and its decay products ^{272}Hs and ^{268}Sg from the ^{232}Th + ^{48}Ca reaction

Yu. Ts. Oganessian,[1] V. K. Utyonkov,[1] M. V. Shumeiko,[1] F. Sh. Abdullin,[1] S. N. Dmitriev,[1] D. Ibadullayev,[1,2] M. G. Itkis,[1] N. D. Kovrizhnykh,[1] D. A. Kuznetsov,[1] O. V. Petrushkin,[1] A. V. Podshibiakin,[1] A. N. Polyakov,[1] A. G. Popeko,[1] I. S. Rogov,[1] R. N. Sagaidak,[1] L. Schlattauer,[1,3] V. D. Shubin,[1] D. I. Solovyev,[1] Yu. S. Tsyganov,[1] A. A. Voinov,[1] V. G. Subbotin,[1] N. S. Bublikova,[1] M. G. Voronyuk,[1] A. V. Sabelnikov,[1] A. Yu. Bodrov,[1,4] Z. G. Gan,[5] Z. Y. Zhang,[5] M. H. Huang,[5] and H. B. Yang[1,5]

[1] *Joint Institute for Nuclear Research, RU-141980 Dubna, Russian Federation*
[2] *L.N. Gumilyov Eurasian National University, 010000 Astana, Kazakhstan*
[3] *Palacky University Olomouc, Department of Experimental Physics, Faculty of Science, 771 46 Olomouc, Czech Republic*
[4] *Lomonosov Moscow State University, Department of Chemistry, Radiochemistry division, RU-119991 Moscow, Russian Federation*
[5] *Institute of Modern Physics, Chinese Academy of Sciences, Lanzhou 730000, China*

(Received 12 July 2023; accepted 28 July 2023; published 23 August 2023)

The ^{232}Th + ^{48}Ca reaction has been studied at the gas-filled separator DGFRS-2 online to the cyclotron DC280 at the SHE Factory at JINR. Three new nuclides were synthesized for the first time: a spontaneously fissioning (SF) ^{268}Sg with the half-life $T_{\mathrm{SF}} = 13^{+17}_{-4}$ s; an α decaying ^{272}Hs with $T_\alpha = 0.16^{+0.19}_{-0.06}$ s and $E_\alpha = 9.63 \pm 0.02$ MeV; and ^{276}Ds with $T_{1/2} = 0.15^{+0.10}_{-0.04}$ ms, $E_\alpha = 10.75 \pm 0.03$ MeV, and an SF branch of 57%. The decay properties of these nuclei are in agreement with the systematics of experimental partial half-lives and α-decay energies of heavy known nuclei, as well as spontaneous-fission half-lives. The cross sections of the $4n$-evaporation channel of $0.07^{+0.17}_{-0.06}$ pb, $0.7^{+1.1}_{-0.5}$ pb, and $0.11^{+0.46}_{-0.09}$ pb were measured at 231, 238, and 251 MeV, respectively.

DOI: 10.1103/PhysRevC.108.024611

I. INTRODUCTION

The experiments and results presented in this article belong to the program of the synthesis and study of the decay properties of the heaviest nuclei at the SHE Factory at JINR [1]. A significant increase in luminosity, verified in earlier experiments with the isotopes Fl ($Z = 114$) and Mc ($Z = 115$) [2–4], allows us to move to the region of very small cross sections down to dozens of femtobarns. This enables us to expand the field of study of the heaviest nuclei and to observe the rare channels of their decay that were previously inaccessible.

Of particular interest are the isotopes of element 110 (Ds). At present, the properties of eight isotopes of Ds with the number of neutrons from 159 to 171 are known. The light isotopes $^{269-271,273}$Ds ($N = 159$–161, 163) were synthesized in cold-fusion reactions. The chains of successive α decays [5,6] led to the known nuclei, which determined their identification. According to the macroscopic-microscopic theory, the closed deformed shells $Z = 108$ and $N = 162$ play a decisive role in the probabilities of their α decay and spontaneous fission (SF).

In hot fusion reactions induced by ^{48}Ca ions, Ds isotopes were obtained many times, but only as daughter nuclei in the synthesis of nuclides with atomic numbers 112, 114, and 116 [7,8]. The Ds isotopes obtained in this way, $^{277,279-281}$Ds ($N = 167$, 169–171), have on average about nine more neutrons than isotopes produced in cold-fusion reactions. They are located away from the deformed shells $Z = 108$ and $N = 162$. Their decay properties are largely determined by the spherical shells $Z = 114$ and $N = 184$, also predicted by the macroscopic-microscopic model. The half-life of neutron-rich isotopes, as expected, increased by more than 3 orders of magnitude for α decay, and the SF becomes a dominant decay mode for the heaviest isotopes with $N = 169$–171.

Of particular interest is the intermediate region of nuclei between the closed shells mentioned above, where the stabilizing effect is minimal. Such nuclides can be synthesized in hot fusion reactions of ^{232}Th, ^{233,235}U targets with ^{48}Ca and ^{40}Ar projectiles. Compared to the known data obtained with the ^{48}Ca beam and heavier targets, a significant decrease in the half-life is expected for the products of these reactions, as well as a considerable loss of fusion-evaporation reaction products caused by the low survival of the compound nuclei with a low fission barrier [9,10].

Previously, several attempts to synthesize Ds isotopes were made in the ^{235}U + ^{40}Ar [11], ^{236}U + ^{40}Ar [12], ^{238}U + ^{40}Ar [13], and ^{232}Th + ^{48}Ca [14] reactions. However, in these experiments, only the upper limits of the cross sections at the level of 8–10 pb were obtained for the evaporation residues (ER). In the most sensitive experiment ^{233}U(^{48}Ca xn) $^{281-x}$Cn, the upper limit of the cross section $\sigma \leqslant 0.6$ pb [15] was also obtained. Now we are returning to this region of nuclei again at the SHE Factory, using its large reserve for the luminosity of the experiment.

In the ^{48}Ca-induced fusion reactions with actinide target nuclei used for the synthesis of superheavy elements, the compound nuclei with $Z = 112$–118 cross the "island of stability" predicted by theory in its northwestern part. The Ds isotopes

 ©2023 American Physical Society

TABLE I. The ^{232}Th target thickness, laboratory-frame energies of ^{48}Ca in the middle of the target layer, resulting excitation energy intervals (with use of mass tables [17,18]), total beam doses, the numbers of observed decay chains assigned to ^{277}Ds ($3n$) and ^{276}Ds ($4n$), and the cross sections of their production.

Target thickness (mg/cm^2)	E_{lab} [a] (MeV)	E^* (MeV)	Beam dose $\times 10^{19}$	No. of chains $3n$ / $4n$	σ_{3n} (pb)	σ_{4n} (pb)
0.89	231.1	32.3-36.6	2.4	0 / 1	< 0.2	$0.07^{+0.17}_{-0.06}$
0.76	237.8	37.9-42.1	1.9	0 / 5	< 0.5	$0.7^{+1.1}_{-0.5}$
0.65	250.6	48.9-52.3	2.0	0 / 1	–	$0.11^{+0.46}_{-0.09}$

[a]The beam energy was measured with a time-of-flight system, which has a systematic uncertainty of 1 MeV.

of interest are located where an ascent to the "island" begins. Their formation cross sections and decay properties, together with the Og isotope data, define the boundaries for the production of nuclei on the island and demonstrate the role of the effect of new nuclear shells in the stability of superheavy nuclides.

II. EXPERIMENT

The present studies were performed at three ^{48}Ca beam energies at the gas-filled separator DGFRS-2 [16] online to the new cyclotron DC280 at the SHE Factory at JINR [1]. Some parameters of the experiments, as well as a number of the observed nuclei and cross sections of their production in the $^{232}\text{Th} + {}^{48}\text{Ca}$ reaction, are listed in Table I.

Similar to Ref. [3], 12 sectors of the target were produced by electrodeposition on a 0.62−mg/cm^2 Ti backing, were mounted on a disk 24 cm in diameter, which was rotated at 980 rpm. To control the thickness of the target layer during the experiment, about 30 μg of ^{243}Am were added to the target as a marker. This made it possible to register periodically the 5.3-MeV α particles of ^{243}Am by the focal detector after a corresponding setting of the DGFRS-2 magnets.

In the first run, the beam intensity was gradually increased up to 4 p μA. The measurements of the α-particle activity of ^{243}Am showed that at the end of the experiment, after collecting a total beam dose of 2.4×10^{19} (see Table I), about 7% of the substance was lost. To avoid damage to the target in the next runs, the beam intensity was reduced to 3 p μA (see also Ref. [3]).

Like in Refs. [2–4], the separator DGFRS-2 was filled with hydrogen at a pressure of 0.9 mbar. The detector chamber was separated from the DGFRS-2 volume by a 0.7-μm Mylar foil and filled with pentane at a pressure of 1.6 mbar. In front of the detectors, two multiwire proportional chambers were installed to register nuclei arriving from the separator.

The focal detector consisted of two 48×128−mm^2 double-sided strip detectors [model BB17 (DS)-300] with 48 1-mm horizontal strips on the front side and 128 1-mm-wide vertical strips on the back one. The first detector shielded a part of the rear detector. The back strips of 1-mm in width were paired together to form 110 strips of 2 mm in width. The focal detector was surrounded by eight 60×120−mm^2 side strip detectors (model W4-300), each with 8 strips, forming a box with a depth of 120 mm. All signals in the detectors with the amplitudes above a threshold of 0.55–0.6 MeV were recorded independently by digital and analog data acquisition systems. The details of the detector system are given in Ref. [16].

III. RESULTS AND DISCUSSION

The energies of α particles or of fission fragments and the decay times of nuclei in the chains observed in these experiments and assigned to the ^{276}Ds parent nucleus are presented in Fig. 1.

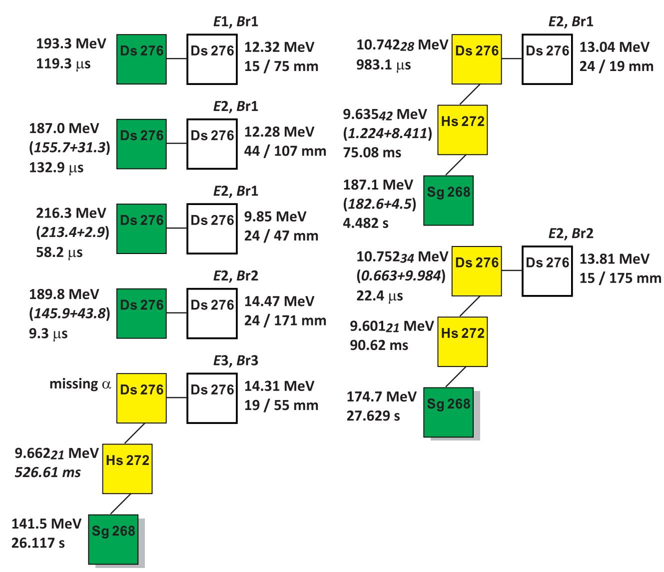

FIG. 1. Decay properties of ^{276}Ds, ^{272}Hs, and ^{268}Sg. The upper rows for each chain show the ^{48}Ca energy ($E1 = 231.1$ MeV, $E2 = 237.8$ MeV, $E3 = 250.6$ MeV) and the separator magnetic rigidity ($B\rho 1 = 2.417$ T m, $B\rho 2 = 2.449$ T m, $B\rho 3 = 2.434$ T m) (on the top of the blank square with a mark "Ds 276"); see text. On the right side of the square, the ER energy and vertical and horizontal positions on the detector (in mm) are given. The rows on the left side provide the α-particle [in yellow (light gray)] and SF-fragment [in green (dark gray)] energies and time intervals between the events. The energies of the summed signals are given in parentheses. The events marked with a shadow were registered during the beam-off periods; see Refs. [2–4]. The α-particle energy errors are shown by smaller italic numbers. The time interval for an α particle following a "missing α" was measured from a preceding ER event and is shown in italic.

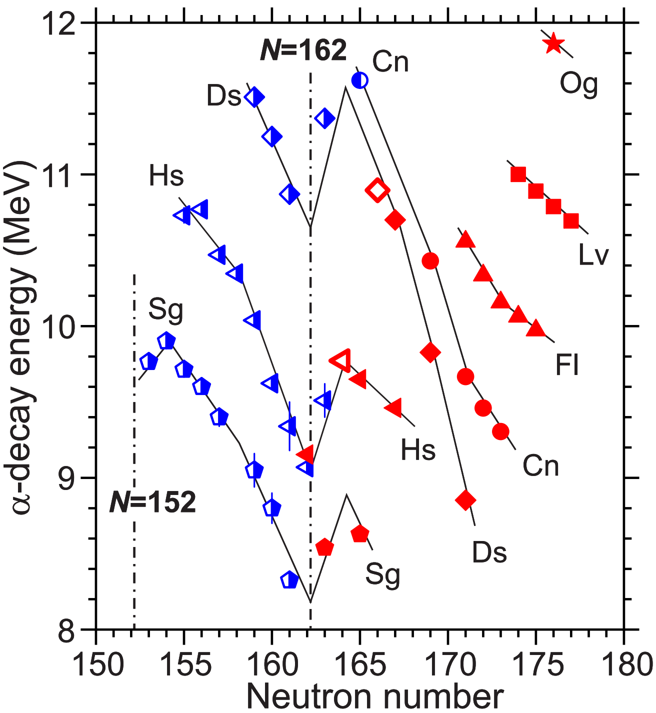

FIG. 2. Alpha-decay energy vs neutron number for the isotopes of elements Sg–Og (red full and blue half-filled symbols refer to nuclei produced in the reactions Ra–Cf + ^{48}Ca and other reactions, respectively). The main part of the data is taken from Ref. [22]; see also Refs. [2–8,15,19–21] and references therein. Open symbols show the results of this work. The lines are drawn to guide the eye.

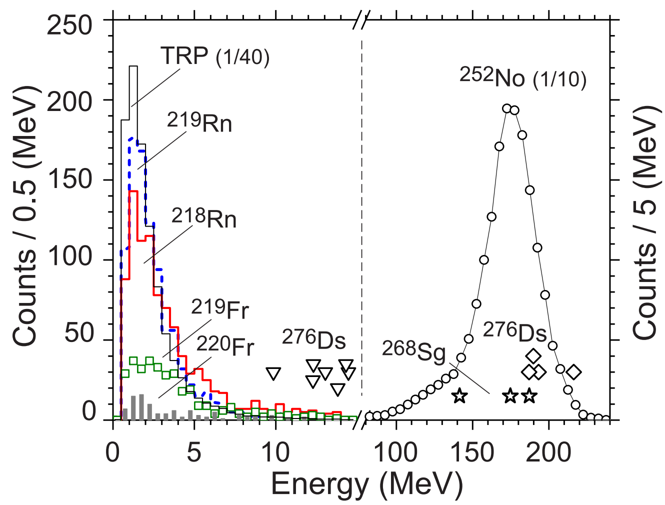

FIG. 3. Energy spectra of recoils within an energy interval of 0–15 MeV and fission fragments with the energies of 80–240 MeV. The black solid histogram (upper) shows a summary spectrum (reduced by a factor of 40) of the recoils of transfer reaction products with $E_\alpha = 6.5$–9.0 MeV and $\Delta t_{R-\alpha} = 0$–5 s. The spectra of ^{219}Rn, ^{218}Rn, ^{219}Fr, and ^{220}Fr recoils are shown with correspondingly smaller yields by the blue dash and red solid histograms, green squares, and the gray histogram, respectively. The ER energies of ^{276}Ds are shown by triangles. The distribution of the SF fragment energies of ^{252}No [16] (reduced by a factor of 10) and the energies of ^{276}Ds and ^{268}Sg are shown by circles, diamonds, and stars, respectively.

The decay properties of nuclei in the three chains with two consecutive α decays terminated by spontaneous fission (Fig. 1) differ from the properties of known nuclei and could not originate from the $3n$ and $5n$ channels of the ^{232}Th + ^{48}Ca reaction because their decay properties do not agree with the data obtained for ^{277}Ds and ^{271}Hs and their descendants, namely: ^{277}Ds ($T_\alpha = 3.5\,^{+2.1}_{-0.9}$ ms, $E_\alpha = 10.55 \pm 0.04$MeV), ^{273}Hs ($T_\alpha = 0.51\,^{+0.30}_{-0.14}$ s, $E_\alpha = 9.51 \pm 0.04$ MeV), ^{269}Sg ($T_\alpha = 14^{+10}_{-4}$ min, $E_\alpha = 8.41 \pm 0.04$ MeV) [19,20] and ^{271}Hs ($T_{1/2} \approx 4$ s, $E_\alpha = 9.13 \pm 0.05$, 9.30 ± 0.05 MeV), ^{267}Sg ($E_\alpha = 8.20 \pm 0.05$ MeV, $b_{\alpha/\mathrm{SF}} = 0.17/0.83$, $T_{1/2} = 80\,^{+60}_{-20}$ s) [21].

The most reasonable explanation for these chains is the product of the $4n$ reaction channel, isotope ^{276}Ds, and its decay products, ^{272}Hs and ^{268}Sg. This statement is based on several arguments. First, in Fig. 2, we show the dependence of α-decay energies vs neutron number $Q_\alpha(N)$ for nuclei from Sg to Og. The Q_α values for the isotopes ^{276}Ds and ^{272}Hs are in good agreement with those expected from the $Q_\alpha(N)$ dependence. In addition, the registered energies of recoils, the half-lives of the observed nuclei, as well as the production cross section of the new nucleus depending on the ^{48}Ca energy, fully correspond to the values that can be expected for ^{276}Ds (see below).

In addition to the three ER-α-α-SF chains, we registered four ER-SF chains shown in Fig. 1. The nonrandom origin of these correlations follows from the absence of other recoils in the corresponding strips for at least 10^3s preceding to SF events. In addition to these SF fragments, one more event with an energy above 100 MeV ($E = 104.8$ MeV) was registered by the focal detector only. No other events were detected in the same strips during previous 10^3s.

The identification of unknown spontaneously fissioning nuclei requires separate consideration. The main source of the recoil-SF background is SF isomers of light actinides [17,23], which can be formed in the incomplete fusion of ^{48}Ca and ^{232}Th nuclei. Despite the low isomeric ratio for these nuclides and the high suppression of incomplete fusion products by the separator, it is not excluded that very rare events of SF isomers can reach the focal detector. However, it is known that SF isomers have a mass-asymmetric spontaneous fission with a relatively low kinetic energy of fission fragments. The kinematics of such reactions differs from that for complete fusion reactions. We used these differences to select the true SF evaporation residues from other products.

The recoil energies in the ER-SF chains observed in the first two runs (see Fig. 1) are shown in Fig. 3. For comparison, we have also given the energy spectra of the transfer reaction products (TRP). Various TRP with $E_\alpha = 6.5$–9.0 MeV and decay times $\Delta t_{\mathrm{R}-\alpha}$ up to 5 s could be easily distinguished by correlations with preceding recoils. To identify several nuclei (^{218}Rn, ^{219}Rn, ^{219}Fr, and ^{220}Fr), we searched for R-α-α correlations.

It can be seen that the energy spectra of all TRP are similar and have a maximum distribution at low energies. The recoil

TABLE II. Summary decay properties of nuclei synthesized in present studies. The first three columns show nucleus, decay mode, and branch, as well as half-life. The next four columns show α-particle energy E_α, α-decay energy Q_α, and partial half-lives with respect to α decay and SF.

Nucleus	Decay mode, branch (%) [a,b]	Half-life [b]	E_α (MeV) [c]	Q_α (MeV) [c]	T_α [b]	T_{SF} [b]
^{276}Ds	SF: 57^{+15}_{-18}	$0.15^{+0.10}_{-0.04}$ ms	10.746(28)	10.904(28)	$0.36^{+0.32}_{-0.15}$ ms	$0.27^{+0.23}_{-0.10}$ ms
^{272}Hs	α	$0.16^{+0.19}_{-0.06}$ s	9.628(21)	9.772(21)		
^{268}Sg	SF	13^{+17}_{-4} s				

[a]Branch is given for the most probable decay mode (α or SF). The branching ratio is not listed when only one decay mode was observed.
[b]Error bars correspond to 68%-confidence level.
[c]Energy uncertainties (standard deviations) given in parentheses correspond to the data with the best energy resolution.

energies of the SF isomers observed in the reaction with ^{242}Pu [3] ($E_R = 0.9$–4.3 MeV) are in good agreement with the given energy distribution of the TRP recoils measured in this experiment. On the contrary, the recoil energies in the chains shown in Fig. 1 are higher and located in the measured kinetic energy region expected for the evaporation residues, e.g., $E_R \geqslant 8.5$ MeV for ^{286,287}Fl and ^{283}Cn in Ref. [3].

In addition, the kinetic energies of the observed fission fragments are also higher than the average energy of ^{252}No and are inside the energy range of the ^{279}Ds fragments ($E_{\text{focal+side}} \approx 168$–$227$ MeV [3]). Finally, the SF isomer of ^{235}U ($T_{SF} = 3.6$ ms [17] or 11 ms [23]) which is closest to ^{232}Th target nucleus, should be formed with the largest cross section. However, the SF nucleus measured in this work has a much shorter half-life, $T_{SF} = 55^{+51}_{-18}$ μs. Based on the arguments above, it seems unlikely that the four observed decays shown in Fig. 1 originate from an SF isomer.

However, the energies of the recoils and fission fragments are in good agreement with what was observed in the three ER-α-α-SF chains assigned to ^{276}Ds. The lifetimes of this nucleus are also close to the decay times of ^{276}Ds. If we attribute all decay times to one nucleus, then the average half-life will be $0.15^{+0.10}_{-0.04}$ ms. In this case, the standard deviation of the logarithm of the measured decay times [$\sigma(\ln t)_{\exp} = 1.47$] of this nucleus fully satisfies the criterion for a single exponent ($\sigma_{\lim} = 0.48$–1.89) proposed in Ref. [24]. The decay times of ^{272}Hs and ^{268}Sg are also in agreement with this criterion.

Based on the combination of the arguments mentioned above, we attribute all the events shown in Fig. 1 to one nucleus ^{276}Ds.

The decay properties of nuclei in the ^{276}Ds decay chain are given in Table II. The probability that α decay of ^{268}Sg has not been registered in the three chains and the fission belongs to ^{264}Rf is less than 0.05% (the probability of registering an α particle exceeds 92%).

The half-lives T_α of the isotopes of even-Z elements from 106 to 118 relative to α decay, including the data from Table II, are shown in Fig. 4. It demonstrates good agreement of the half-lives of ^{276}Ds and ^{272}Hs with the systematics for the corresponding elements.

The T_{SF} values for ^{276}Ds and ^{268}Sg are in reasonable agreement with the systematics of experimental spontaneous-fission half-lives as well as with the theoretical predictions of T_{SF} [25,26] which rather well reproduce the experimental data for nuclei obtained in the ^{48}Ca-induced reactions, see, e.g., Fig. 3 in Ref. [4]. The T_{SF} values of 2.2 h [25] and 3.5 h [26] for ^{268}Sg and 16 ms [25] and 2.1 s [26] for ^{276}Ds are predicted. After the correction of these values proposed in Ref. [4], they remain somewhat overestimated, but within the limits of the accuracy of such calculations, viz. 30 min [25] and 7 min [26] for ^{268}Sg and 4 ms [25] and 70 ms [26] for ^{276}Ds. Even better agreement with the experimental data is found within a new cluster approach [27], which results in the T_{SF} values of 1.7 s and 0.94 ms for ^{268}Sg and ^{276}Ds, respectively, compare with $T_{SF} = 13$ s and 0.27 ms for these isotopes given in Table II. Thus, the experimental T_{SF} values are in reasonable agreement with theoretical models.

The production cross sections for ^{276}Ds in the ^{232}Th + ^{48}Ca reaction are shown in Fig. 5. The cross sections of the ^{242}Pu + ^{48}Ca [3,15,19], ^{238}U + ^{48}Ca [3,15,28,29], and ^{226}Ra + ^{48}Ca [30] reactions are given for comparison. As

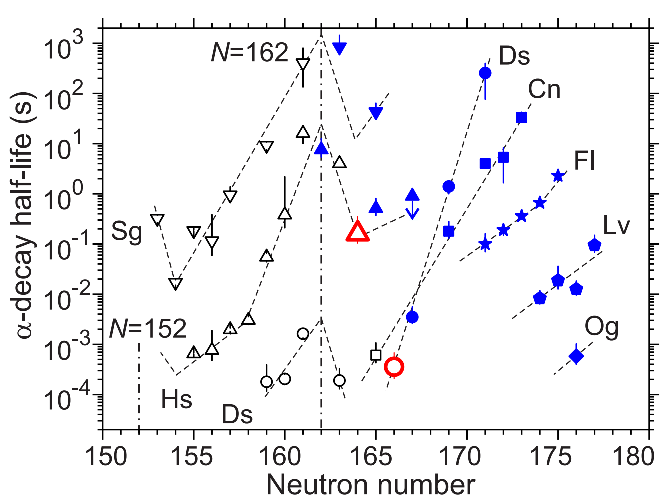

FIG. 4. Partial half-lives T_α vs neutron number for the isotopes of even-Z elements with Z = 106–118. The results from the Ra–Cf + ^{48}Ca reactions are shown by full blue symbols; the results for ^{276}Ds and ^{272}Hs from this work are shown by a red open circle and a triangle (large symbols), respectively; other data are shown by black open symbols; see Refs. [2–8,17,19–21] and references therein. The lines are drawn to guide the eye.

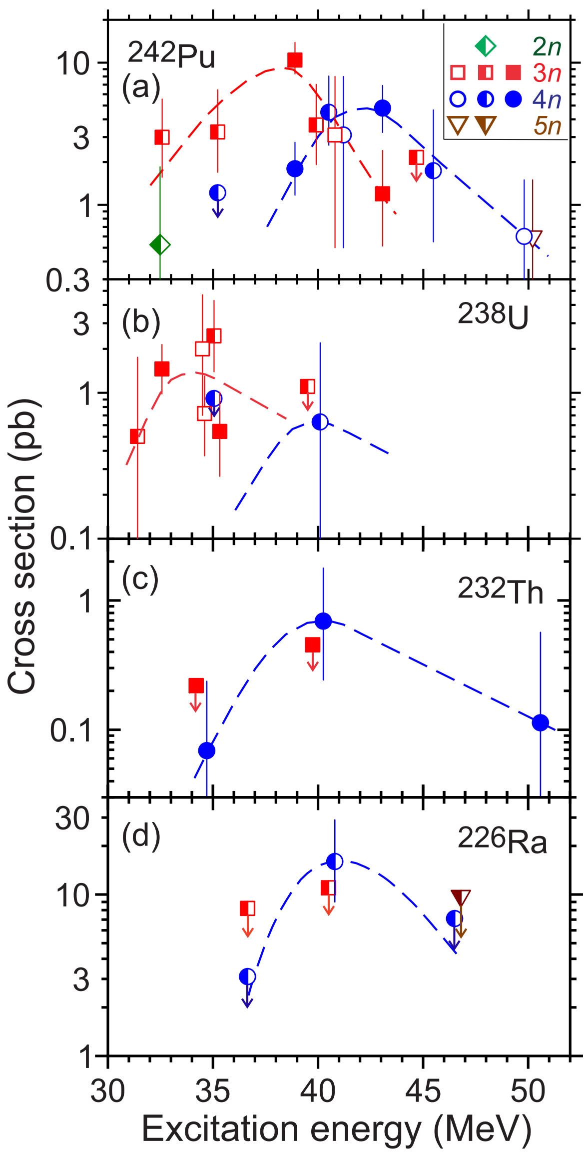

FIG. 5. Cross sections for the 2n- to 5n-evaporation channels for the ^{242}Pu (a), ^{238}U (b), ^{232}Th (c), ^{226}Ra + ^{48}Ca (d) reactions. Vertical error bars correspond to total uncertainties. The symbols with arrows show the upper cross-section limits. The data are shown by open (from Refs. [19,28,29]), half-closed (from Refs. [15,30]), and closed symbols (from Ref. [3] and this work). The dashed lines through the data are drawn to guide the eye.

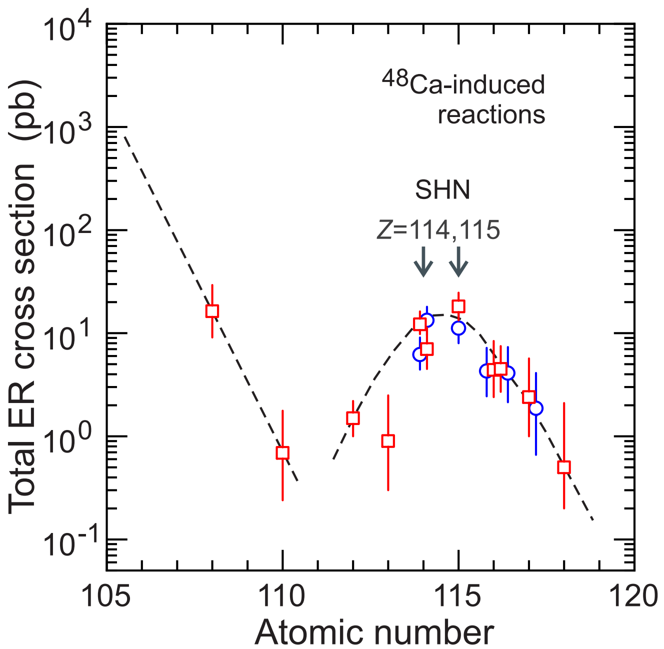

FIG. 6. Maximum production cross sections for the isotopes of heavy elements in the ^{48}Ca-induced reactions with ^{226}Ra, ^{232}Th, ^{238}U, ^{242,244}Pu, ^{243}Am, ^{245,248}Cm, ^{249}Bk, and ^{249}Cf. Data measured at DGFRS and DGFRS-2 are shown by red squares (Refs. [2–4,7,15,30] and this work), the results obtained at SHIP, BGS, TASCA, and GARIS are shown by blue circles [19,32–36]. The lines are drawn to guide the eye.

could be expected [9,10,31], the differences in the fission barriers and neutron binding energies affect the survival probability. The measured maximum cross section of the fusion-evaporation reaction ^{232}Th + ^{48}Ca is smaller than the cross sections of the reactions with ^{226}Ra, ^{238}U, and ^{242}Pu.

One may note that in the reactions with ^{242}Pu and ^{238}U, the measured cross sections of the 3n-evaporation channel exceed the yields of the 4n-channel products. In the reaction with ^{232}Th, we did not observe the 3n-evaporation channel. In the ^{226}Ra + ^{48}Ca reaction [30], the products of this channel were not observed either, although in the ^{248}Cm + ^{26}Mg reaction, the cross section of the 3n channel was comparable to the maxima of the 4n and 5n channels. This suppression of the 3n channel in reactions with lighter target nuclei can be explained, e.g., by their smaller static deformations, which can lead to a decrease in the capture cross-sections for these reactions at the fusion barrier [21,31].

The cross sections for the formation of the heaviest elements (the maximum of the total cross section of the xn – channels) are shown in Fig. 6. The data were obtained during the synthesis of elements with $Z = 108$ and 112–118 in the fusion reactions of target nuclei ^{226}Ra, as well as ^{238}U, ^{237}Np, ^{242,244}Pu, ^{243}Am, ^{245,248}Cm, ^{249}Bk, and ^{249}Cf, with ^{48}Ca projectiles. Now they are complemented for the first time with data on the synthesis of the new isotope of element 110 in the ^{232}Th + ^{48}Ca reaction. The isotope ^{276}Ds is formed with a cross section an order of magnitude lower than that for the lighter nuclide ^{270}Hs ($N = 162$) in the ^{226}Ra (^{48}Ca, 4n) ^{270}Hs reaction [30]. On the contrary, when moving to the region of heavier elements ($Z > 110$), the cross section increases.

Such variation is in full agreement with theoretical models predicting the closed shells at $Z = 108$, $N = 162$ and $Z = 114$, $N = 184$. At the mass limits of the atomic nuclei, the effect of these shells significantly increases the survival of the heaviest compound nuclei and thus determines the existence of superheavy elements. In this regard, a significant rise in the cross section from Ds to the isotopes of Fl and Mc, observed in fusion reactions with ^{48}Ca, is essentially an ascent to the "island of stability" and a step toward the magic numbers at $Z = 114$ and $N = 184$, see, e.g., Ref. [37] and references therein.

IV. SUMMARY

The $^{232}Th + ^{48}Ca$ reaction has been studied at three projectile energies at the new separator DGFRS-2. Three new superheavy nuclides ^{268}Sg, ^{272}Hs, and ^{276}Ds were synthesized for the first time.

To validate further the identification of new nuclei, their observed decay properties were compared with the properties of the transfer reaction products, the systematics of experimental partial half-lives and α decay energies of heavy known nuclei, as well as with the spontaneous-fission half-lives.

The production cross section for ^{276}Ds, obtained in fusion of ^{232}Th and ^{48}Ca nuclei compared to the synthesis of all transactinides with $Z = 108$–118 in the ^{48}Ca-induced reactions turned out to be the smallest one or close to that for ^{294}Og.

This agrees with the predicted heights of the fission barriers and the neutron binding energies of nuclei formed in the process of sequential emission of four neutrons from the ^{280}Ds compound nucleus.

During the experiment with ^{48}Ca and ^{232}Th target lasting less than a month, a sensitivity of about 70 fb was achieved, which indicates a strong potential for the research of superheavy nuclei with low production cross sections.

ACKNOWLEDGMENTS

We thank the personnel operating the DC280 cyclotron and the associates of the ion-source group for obtaining ^{48}Ca beams. We thank K. Rykaczewski for helpful discussions and suggestions. These studies were supported by the Ministry of Science and Higher Education of the Russian Federation through Grant No. 075-10-2020-117 and by the JINR Directorate grant. This work was also supported by the Strategic Priority Research Program of Chinese Academy of Sciences (Grant No. XDB34010000).

[1] G. G. Gulbekian *et al.*, Start-up of the DC-280 cyclotron, the basic facility of the factory of superheavy elements of the laboratory of nuclear reactions at the joint institute for nuclear research, Phys. Part. Nucl. Lett. **16**, 866 (2019).

[2] Yu. Ts. Oganessian *et al.*, First experiment at the superheavy element factory: High cross section of ^{288}Mc in the $^{243}Am + ^{48}Ca$ reaction and identification of the new isotope ^{264}Lr, Phys. Rev. C **106**, L031301 (2022).

[3] Yu. Ts. Oganessian *et al.*, Investigation of ^{48}Ca-induced reactions with ^{242}Pu and ^{238}U targets at the JINR superheavy element factory, Phys. Rev. C **106**, 024612 (2022).

[4] Yu. Ts. Oganessian *et al.*, New isotope ^{286}Mc produced in the $^{243}Am + ^{48}Ca$ reaction, Phys. Rev. C **106**, 064306 (2022).

[5] S. Hofmann, Superheavy elements, Lect. Notes Phys. **764**, 203 (2009).

[6] T. Sumita *et al.*, New result on the production of ^{277}Cn by the $^{208}Pb + ^{70}Zn$ reaction, J. Phys. Soc. Jpn. **82**, 024202 (2013).

[7] Yu. Ts. Oganessian and V. K. Utyonkov, Superheavy nuclei from ^{48}Ca-induced reactions, Nucl. Phys. A **944**, 62 (2015).

[8] A. Såmark-Roth *et al.*, Spectroscopy Along Flerovium Decay Chains: Discovery of ^{280}Ds and an Excited State in ^{282}Cn, Phys. Rev. Lett. **126**, 032503 (2021).

[9] P. Jachimowicz, M. Kowal, and J. Skalski, Properties of heaviest nuclei with $98 \leqslant Z \leqslant 126$ and $134 \leqslant N \leqslant 192$, At. Data Nucl. Data Tables **138**, 101393 (2021).

[10] P. Möller, A. J. Sierk, T. Ichikawa, and H. Sagawa, Nuclear ground-state masses and deformations: FRDM (2012), At. Data Nucl. Data Tables **109–110**, 1 (2016).

[11] G. Münzenberg *et al.*, An attempt to synthesize element 110 in the reaction $^{40}Ar + ^{235}U$, GSI Annual Report 1986 GSI-87-1 (GSI Helmholtzzentrum für Schwerionenforschung, Darmstadt, Germany, 1987), p. 14.

[12] Yu. Ts. Oganessian, Yu. V. Lobanov, A. G. Popeko, F. Sh. Abdullin, G. G. Gulbekiayan, Yu. P. Kharitonov, A. A. Ledovskoy, S. P. Tretyakova, Yu. S. Tsyganov, and V. E. Zhuchko, An attempt to synthesize element 110 in the reaction $^{40}Ar + ^{236}U$ and to identify it using a gas-filled separator, in Proceedings of the 6th International Conference on Nuclei Far from Stability and 9th International Conference on Atomic Masses and Fundamental Constants. Bernkastel-Kues, Germany (1992). Inst. Phys. Conf., Vol. **132** (1993), pp. 429–432.

[13] Yu. A. Lazarev *et al.*, A domain of nuclear stability around shell closures $N = 162$ and $Z = 108$ discovered by identification of the new nuclides $^{262}104$, $^{265,266}106$, $^{267}108$, and $^{273}110$, Heavy ion physics, Scientific Report 1993–1994, JINR Report No. E7-95-227 (JINR, Dubna, 1995), pp. 29–34.

[14] Yu. Ts. Oganessian *et al.*, Experiments on the synthesis of superheavy elements with $Z = 110$, 112 via ^{232}Th, $^{238}U + ^{48}Ca$ reactions, Acta Phys. Slov. **49**, 65 (1999).

[15] Yu. Ts. Oganessian *et al.*, Measurements of cross sections and decay properties of the isotopes of elements 112, 114, and 116 produced in the fusion reactions $^{233,238}U$, ^{242}Pu, and $^{248}Cm + ^{48}Ca$, Phys. Rev. C **70**, 064609 (2004).

[16] Yu. Ts. Oganessian *et al.*, DGFRS-2 − A gas-filled recoil separator for the Dubna super heavy element factory, Nucl. Instrum. Methods Phys. Res. A **1033**, 166640 (2022).

[17] F. G. Kondev, M. Wang, W. J. Huang, S. Naimi, and G. Audi, The NUBASE2020 evaluation of nuclear physics properties, Chin. Phys. C **45**, 030001 (2021).

[18] W. D. Myers and W. J. Swiatecki, Nuclear properties according to the Thomas-Fermi model, Nucl. Phys. A **601**, 141 (1996).

[19] P. A. Ellison *et al.*, New Superheavy Element Isotopes: $^{242}Pu(^{48}Ca, 5n)^{285}114$, Phys. Rev. Lett. **105**, 182701 (2010).

[20] V. K. Utyonkov *et al.*, Neutron-deficient superheavy nuclei obtained in the $^{240}Pu + ^{48}Ca$ reaction, Phys. Rev. C **97**, 014320 (2018).

[21] J. Dvorak *et al.*, Doubly Magic Nucleus $^{270}_{108}Hs_{162}$, Phys. Rev. Lett. **97**, 242501 (2006); Observation of the $3n$ Evaporation Channel in the Complete Hot-Fusion Reaction $^{26}Mg + ^{248}Cm$ Leading to the New Superheavy Nuclide ^{271}Hs, **100**, 132503 (2008).

[22] M. Wang, W. J. Huang, F. G. Kondev, G. Audi, and S. Naimi, The Ame2020 atomic mass evaluation (II). Tables, graphs and references, Chin. Phys. C **45**, 030003 (2021).

[23] S. Garg, B. Maheshwari, B. Singh, Y. Sun, A. Goel, and A. K. Jain, Atlas of Nuclear Isomers, Second Edition, At. Data Nucl. Data Tables **150**, 101546 (2023).

[24] K. H. Schmidt, A new test for random events of an exponential distribution, Eur. Phys. J. A **8**, 141 (2000).

[25] Z. Łojewski and A. Staszczak, Role of pairing degrees of freedom and higher multipolarity deformations in spontaneous fission process, Nucl. Phys. A **657**, 134 (1999).

[26] R. Smolańczuk, J. Skalski, and A. Sobiczewski, Spontaneous fission half-lives of deformed superheavy nuclei, Phys. Rev. C **52**, 1871 (1995).

[27] I. S. Rogov, G. G. Adamian, and N. V. Antonenko, Cluster approach to spontaneous fission of even-even isotopes of U, Pu, Cm, Cf, Fm, No, Rf, Sg, and Hs, Phys. Rev. C **104**, 034618 (2021); Spontaneous fission hindrance in even-odd nuclei within a cluster approach, **105**, 034619 (2022).

[28] S. Hofmann *et al.*, The reaction ^{48}Ca + ^{238}U $\rightarrow$ ^{286}112* studied at the GSI-SHIP, Eur. Phys. J. A **32**, 251 (2007).

[29] D. Kaji, K. Morimoto, H. Haba, Y. Wakabayashi, M. Takeyama, S. Yamaki, Y. Komori, S. Yanou, S.-i. Goto, and K. Morita, Decay measurement of ^{283}Cn produced in the ^{238}U(^{48}Ca,3n) reaction using GARIS-II, J. Phys. Soc. Jpn. **86**, 085001 (2017).

[30] Yu. Ts. Oganessian *et al.*, Synthesis and study of decay properties of the doubly magic nucleus ^{270}Hs in the ^{226}Ra + ^{48}Ca reaction, Phys. Rev. C **87**, 034605 (2013).

[31] J. Hong, G. G. Adamian, N. V. Antonenko, M. Kowal, and P. Jachimowicz, Isthmus connecting mainland and island of stability of superheavy nuclei, Phys. Rev. C **106**, 014614 (2022); G. G. Adamian (private communication).

[32] J. M. Gates *et al.*, First superheavy element experiments at the GSI recoil separator TASCA: The production and decay of element 114 in the ^{244}Pu (^{48}Ca, 3$-$4n) reaction, Phys. Rev. C **83**, 054618 (2011).

[33] S. Hofmann *et al.*, The reaction ^{48}Ca + ^{248}Cm $\rightarrow$ ^{296}116* studied at the GSI-SHIP, Eur. Phys. J. A **48**, 62 (2012).

[34] U. Forsberg *et al.*, Recoil-α-fission and recoil-α-α-fission events observed in the reaction ^{48}Ca + ^{243}Am, Nucl. Phys. A **953**, 117 (2016).

[35] D. Kaji *et al.*, Study of the reaction ^{48}Ca + ^{248}Cm $\rightarrow$ ^{296}Lv* at RIKEN-GARIS, J. Phys. Soc. Jpn. **86**, 034201 (2017).

[36] J. Khuyagbaatar *et al.*, Fusion reaction ^{48}Ca + ^{249}Bk leading to formation of the element Ts (Z = 117), Phys. Rev C **99**, 054306 (2019).

[37] P. Möller, The most important theoretical developments leading to the current understanding of heavy-element stability, Eur. Phys. J. A **59**, 77 (2023).